Limited Recharge of a Steady Deep Groundwater Aquifer in the Southern Highlands of Early Mars

Eric Hiatt[1], Mohammad Afzal Shadab[1], Sean P. S. Gulick[1], Timothy Andrew Goudge[1], and Marc Hesse[1]

[1]University of Texas at Austin

December 7, 2022

Abstract

To determine plausible groundwater recharge rates on early Mars, we develop analytic and numerical solutions for an unconfined steady-state aquifer beneath the southern highlands. We show that the aquifer's mean hydraulic conductivity, K, is the primary constraint on the plausible magnitude of mean steady recharge, r. By restricting groundwater upwelling to Arabia Terra, using a mean hydraulic conductivity of, K ${\sim}10^{-7}$ m/s, and varying shoreline elevations and recharge distributions, the mean recharge must be order of 10^{-2} mm/yr. Recharge for other values of K can be estimated as r ${\sim}10^{-5}\,K$. Our value is near the low end of previous recharge estimates and two orders-of-magnitude below the smallest precipitation estimates. This suggests that, for a steady hydrologic cycle, most precipitation forms runoff, not groundwater recharge. It is also plausible the transient aquifer response to recharge is sufficiently slow that no upwelling occurs prior to cessation of climatic excursions causing precipitation.

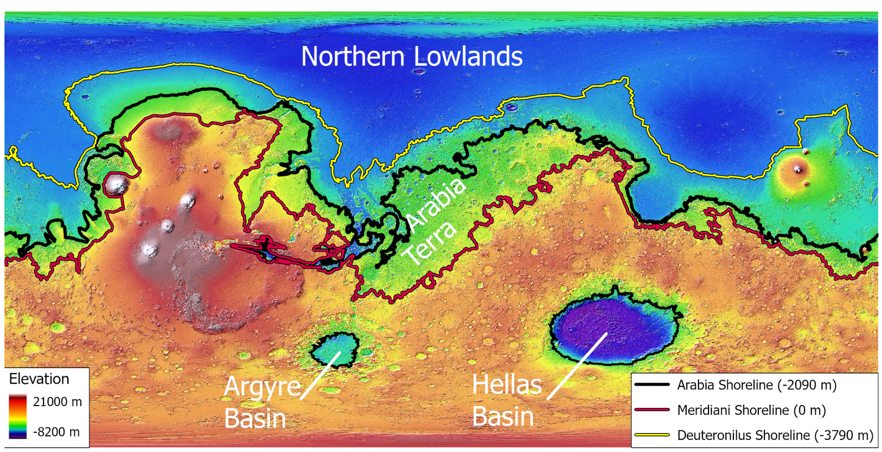

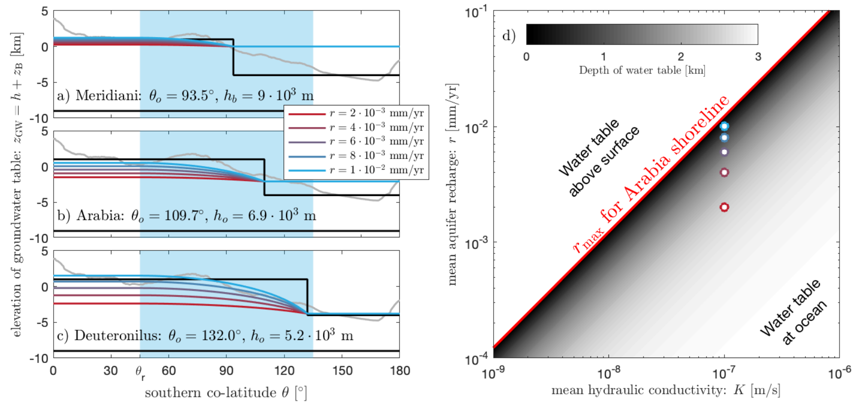
a) Meridiani: $\theta_o = 93.5^\circ$, $h_b = 9 \cdot 10^3$ m
b) Arabia: $\theta_o = 109.7^\circ$, $h_o = 6.9 \cdot 10^3$ m
c) Deuteronilus: $\theta_o = 132.0^\circ$, $h_o = 5.2 \cdot 10^3$ m
$r = 2 \cdot 10^{-3}$ mm/yr
$r = 4 \cdot 10^{-3}$ mm/yr
$r = 6 \cdot 10^{-3}$ mm/yr
$r = 8 \cdot 10^{-3}$ mm/yr
$r = 1 \cdot 10^{-2}$ mm/yr
elevation of groundwater table: $z_{GW} = h + z_B$ [km]
southern co-latitude θ [°]
θ_r
d)
Depth of water table [km]
Water table above surface
r_{max} for Arabia shoreline
Water table at ocean
mean aquifer recharge: r [mm/yr]
mean hydraulic conductivity: K [m/s]

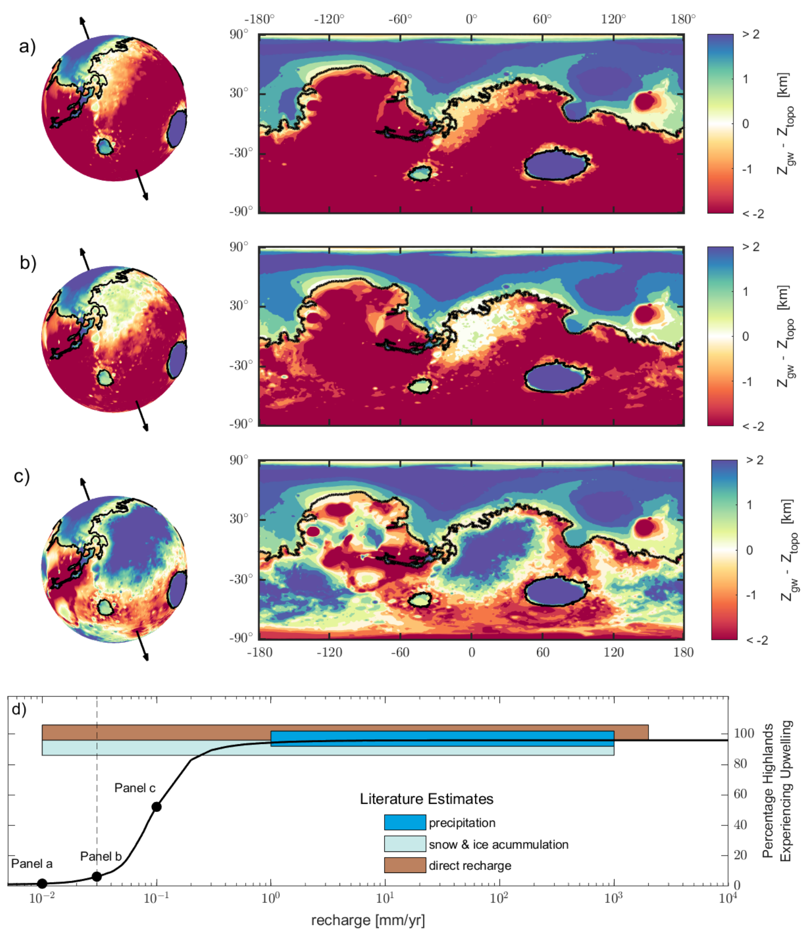
a)
b)
c)
d)
$Z_{gw} - Z_{topo}$ [km]
> 2
< -2
Panel a
Panel b
Panel c
Literature Estimates
precipitation
snow & ice acummulation
direct recharge
Percentage Highlands Experiencing Upwelling
recharge [mm/yr]

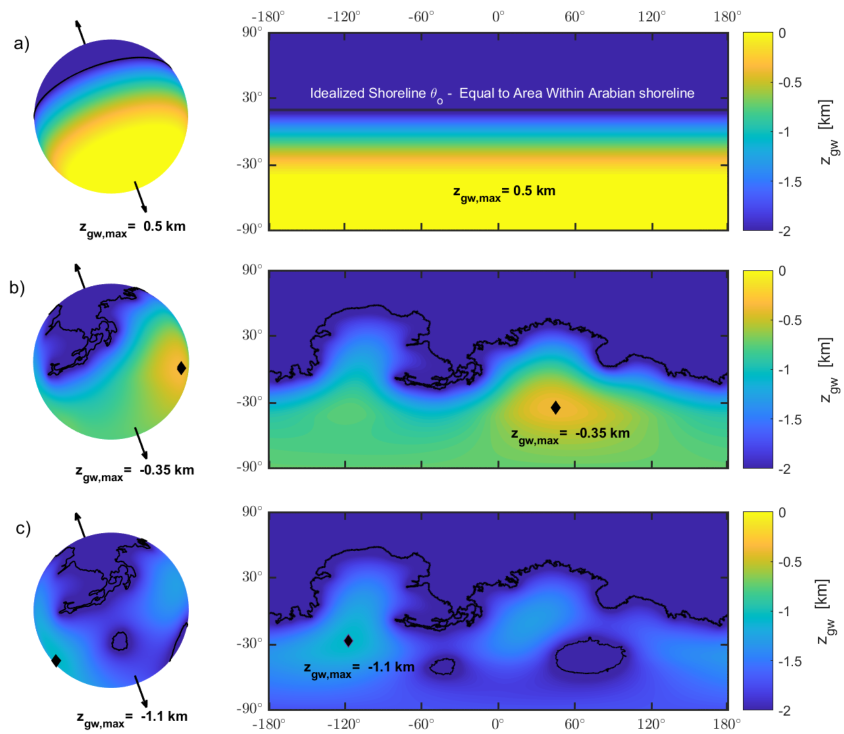

a)
b)
c)
Idealized Shoreline θ_o - Equal to Area Within Arabian shoreline
$z_{gw,max}$ = 0.5 km
$z_{gw,max}$ = -0.35 km
$z_{gw,max}$ = -1.1 km
z_{gw} [km]

Limited Recharge of a Steady Deep Groundwater Aquifer in the Southern Highlands of Early Mars

Eric Hiatt[1,2,3], Mohammad Afzal Shadab[2,3,4], Sean P.S. Gulick[1,2,3], Timothy A. Goudge[1,3,5], Marc A. Hesse[1,4]

[1]Department of Geological Sciences, Jackson School of Geosciences, The University of Texas at Austin
[2]University of Texas Institute for Geophysics, The University of Texas at Austin
[3]Center for Planetary Systems Habitability, The University of Texas at Austin
[4]Oden Institute for Computational Engineering and Sciences, The University of Texas at Austin
[5]CIFAR Azrieli Global Scholars Program, CIFAR, Toronto, Ontario, Canada

Key Points:

- Analytic solution for an unconfined aquifer beneath Mars southern highlands provides first-order estimate of groundwater table elevation.
- The key control on the steady groundwater table elevation is the ratio between mean recharge and mean hydraulic conductivity of the aquifer.
- For commonly assumed values of hydraulic conductivity the steady recharge must be at the lower end of the estimated range of recharge.

Corresponding author: Eric Hiatt, `eric.hiatt@utexas.edu`

Abstract

To determine plausible groundwater recharge rates on early Mars, we develop analytic and numerical solutions for an unconfined steady-state aquifer beneath the southern highlands. We show that the aquifer's mean hydraulic conductivity, K, is the primary constraint on the plausible magnitude of mean steady recharge, r. By restricting groundwater upwelling to Arabia Terra, using a mean hydraulic conductivity of, $K \sim 10^{-7}$ m/s, and varying shoreline elevations and recharge distributions, the mean recharge must be order of 10^{-2} mm/yr. Recharge for other values of K can be estimated as $r \sim 10^{-5}\,K$. Our value is near the low end of previous recharge estimates and two orders-of-magnitude below the smallest precipitation estimates. This suggests that, for a steady hydrologic cycle, most precipitation forms runoff, not groundwater recharge. It is also plausible the transient aquifer response to recharge is sufficiently slow that no upwelling occurs prior to cessation of climatic excursions causing precipitation.

Plain Language Summary

The surface of Mars shows past evidence for liquid water at its surface, however the extent surface water interacted with the subsurface remains an open question. In this work, we derive an idealized mathematical solution for an equation often used to study groundwater flow on Earth and Mars. We use this solution to analyze and validate a computer model based approximation in a global configuration capable of examining several parameters that could act as first-order controls on recharge a possible Martian aquifer. We use topography data along with rover and remotely sensed observations to constrain the model, and find that there is a single parameter, recharge/hydraulic conductivity $\sim 10^{-5}$, that controls the amount of recharge an early Martian aquifer can plausibly sustain with these constraints. This value is far less than predicted by previous literature.

1 Introduction

The surface of Mars retains several planetary scale structures. One of the most striking is the crustal dichotomy separating Mars' northern lowlands from its southern highlands via an abrupt ∼5 km topographic transition. In stark contrast to the relatively smooth plains in the north, the southern highlands preserve the oldest, most heavily cratered terrain on the planet as well as at minimum two large scale impact basins, Hellas and Argyre (Smith et al., 1999). These structures formed prior to ∼3.7 Ga, in the Noachian Era, at a time when Mars is also hypothesized to have had an active hydrologic cycle (Frey, 2008; Werner, 2008; Carr, 1986; Clifford, 1993a). The formation of these structures would have impacted any possible surface and groundwater processes due to their associated topographic lows.

There is ample evidence for liquid water on Mars' surface early in the planet's history. The eroded remains of poorly integrated fluvial drainage systems, called "valley networks", dissect the highlands (Milton, 1973; Goldspiel & Squyres, 1991; Carr, 1996; Hynek & Phillips, 2001). Spectral data strengthens the inference of past surface water processes with observations of hydrated silicates suggesting near surface aqueous mineral alteration (Mustard et al., 2008; Ehlmann et al., 2009; Carter et al., 2013). Open and closed crater lakes have been identified throughout the Noachian terrain, providing further evidence of standing bodies of water on the Martian surface (Cabrol & Grin, 1999; Fassett & Head, 2008b; Di Achille & Hynek, 2010). In both Argyre and Hellas, observations have been made supporting the possible presence of large standing bodies of water (Parker et al., 2000; Wilson et al., 2010; Dohm et al., 2015; Hiesinger & Head, 2002; Hargitai et al., 2018; Zhao et al., 2020). Many have also argued that an immense ocean once existed within the northern lowlands (e.g., Parker et al., 1989, 1993; Carr & Head, 2003; Fassett & Head, 2008a).

Conclusive evidence of surface water processes and standing bodies of water naturally leads to questions regarding the formation and extent of any groundwater systems. A globally connected groundwater system has been inferred in numerous geomorphic and numeric modeling based studies (e.g., Clifford, 1993a; Andrews-Hanna et al., 2007; Di Achille & Hynek, 2010; Salese et al., 2019). Additionally, rover and satellite based observations of layered deposits in Arabia Terra (Figure 1) have been interpreted as evaporites resulting from groundwater upwelling (Christensen et al., 2000; Golombek et al., 2003; Squyres et al., 2004; McLennan et al., 2005; Grotzinger et al., 2005; Bibring et al., 2007; Andrews-Hanna et al., 2007).

To examine the effect of standing bodies of water on possible groundwater tables, here we use mean shoreline elevations at Deuteronilus (-3790 m), Arabia (-2090 m), and Meridiani (0 m) as illustrative examples (see table 1 in Carr & Head (2003)). However, we will show that the existence of a northern ocean, regardless of depth, is a secondary control on groundwater when compared to the geometry of the dichotomy. This is consequential due to the general contention regarding the existence of putative northern ocean(s) (e.g., Malin & Edgett, 1999; Sholes et al., 2019, 2021; Sholes & Rivera-Hernández, 2022). While some studies argue that the kilometer-scale deviation of equipotential shorelines precludes the existence of an ocean, others have suggested that true polar wander and deformation associated with the Tharsis rise can explain these discrepancies (Perron et al., 2007; Citron et al., 2018; Chan et al., 2018).

The contention surrounding the northern ocean dictates our use of less controversial model constraints. The distribution of valley networks offers insight regarding groundwater table elevation. The groundwater table often sets local base level to which sedimentary systems can erode. The widespread distribution of incised valley networks across the highlands implies any groundwater table was likely well below the surface topography over much of the planet. Similarly, Arabia Terra's noticeable lack of incised valley networks and the presence of inverted fluvial deposits along with layered deposits suggests that the region was a depositional environment, with the groundwater table perhaps at or near the surface (Davis et al., 2016) consistent with rover observations in this region (e.g., McLennan et al., 2005; Grotzinger et al., 2005). Parameters such as basin hydraulic head levels and recharge distributions will be compared to these observational constraints.

Published precipitation and aquifer recharge rates vary by orders of magnitude. Estimates of water availability due to snow and ice accumulation give values ranging from 10^{-2} to 10^{3} mm/yr (e.g., Wordsworth et al., 2015; Fastook & Head, 2015; von Paris et al., 2015) and estimates associated with precipitation range from $10^{0}-10^{3}$ mm/yr (e.g., Kamada et al., 2020; Wordsworth et al., 2015). Geomorphic studies have constrained water associated with runoff production between 10^{2} to 10^{5} mm/yr (Ramirez et al., 2020; Hoke et al., 2011). However, these studies only provide an upper bound on groundwater recharge due to the unknown partitioning between surface runoff and infiltration.

Direct estimates of recharge from groundwater modeling studies vary between 10^{-2} to 10^{3} mm/yr, but require the specification of unknown aquifer properties (Harrison & Grimm, 2009; Andrews-Hanna et al., 2007, 2010; Luo et al., 2011; Horvath & Andrews-Hanna, 2017). Here, we individually examine the importance of unknown aquifer properties, the effects of possible standing bodies of water, and consequences associated with varying recharge distributions on the aquifer using novel analytic and numeric groundwater models. By comparing solutions with the inferred upwelling within Arabia Terra and valley network distributions, we ask: what are plausible mean recharge estimates for a steady-state, deep groundwater aquifer on early Mars?

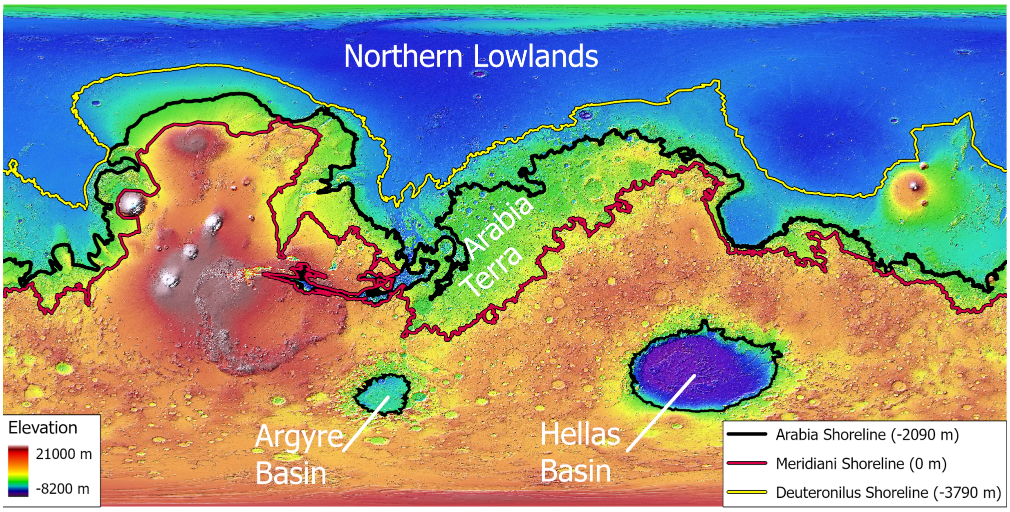

Figure 1. Topography of Mars derived from Mars Orbiter Laser Altimetry (MOLA) aboard the Mars Global Surveyor (MGS) mission (Smith et al., 1999). Hellas and Argyre impact basins are labeled along with the northern lowlands. Three mean shorelines elevations are taken from Parker et al. (1989) and Carr & Head (2003). Argyre and Hellas impact basins are outlined at an elevation of -2090 m.

2 Methodology

2.1 Model for the southern highlands aquifer

Similar to other Mars groundwater studies (Clifford, 1993b; Hanna & Phillips, 2005; Luo & Howard, 2008), we use the Dupuit-Boussinesq model (Dupuit, 1863; Forchheimer, 1901; Boussinesq, 1903) for the elevation, h, of the groundwater table above the base of the aquifer

$$-\nabla \cdot [K\, h \nabla h] = r\, \chi(\theta, \theta_r), \tag{1}$$

where θ is the angle from the south pole or southern colatitude in radians and $\chi(\theta, \theta_r)$ is an indicator function that is one for $\theta_r \leq \theta \leq \pi - \theta_r$ and zero otherwise. The divergence and gradient operators take their standard from in spherical shell coordinates (Batchelor, 2000). We assume the flow is steady to examine the temporally averaged mean recharge rates.

The model has two physical parameters, the mean hydraulic conductivity of the aquifer, K, and the mean recharge rate, r. For clarity of presentation, we assume that K and r are spatially constant, although our analysis can be extended to variable conductivity and recharge. We assume recharge is evenly distributed across an equatorial band of width, $\Delta\theta_r$, between colatitude θ_r and $180° - \theta_r$. Unless otherwise specified, we assume $\theta_r = 45°$, and the head, h, is measured relative to the base of the aquifer, which is assumed to be at an elevation $z_{\mathrm{B}} = -9$ km as in previous studies (Andrews-Hanna et al., 2010; Andrews-Hanna & Lewis, 2011). For a mean elevation of the highlands of $z_{\mathrm{H}} = 1$ km, the aquifer has a maximum thickness of $d = z_{\mathrm{H}} - z_{\mathrm{B}} = 10$ km.

As a boundary condition, the groundwater table at the perimeter of our aquifer is set equal to the mean elevation, z_{o}, of one of the proposed shorelines, $h(\theta_{\mathrm{o}}) = h_o = z_{\mathrm{o}} - z_{\mathrm{B}}$. We use the three shorelines mapped in Figures 2*a*-2*c*. When present in a particular model, shoreline elevations in both Hellas and Argyre are set equal to the dichotomy shoreline being examined in that particular model run.

2.2 Analytic solution for an idealized spherical cap aquifer

We first investigate a one-dimensional model for an idealized spherical cap aquifer. To obtain analytic solutions for the groundwater table, we assume circumferential symmetry so that the solution is only a function of colatitude, θ (Shadab et al., 2022). In this limit, equation (1) reduces to

$$-\frac{1}{R\sin\theta}\frac{\mathrm{d}}{\mathrm{d}\theta}\left[\frac{K}{R}\sin\theta h\frac{\mathrm{d}h}{\mathrm{d}\theta}\right] = r\,\chi(\theta,\theta_r) \quad \text{on} \quad \theta\in[0,\,\theta_\mathrm{o}]\,, \tag{2}$$

where R is the mean radius of Mars, $\sim 3,390$ km (Smith et al., 1999), and θ_o is the southern colatitude of the mean shoreline of the northern ocean. Here we choose θ_o so that the surface area of the idealized spherical-cap aquifer is equivalent to the area enclosed by the shoreline in Figure 1. We assume a simple step in topography at the shoreline, θ_o, between the mean highland elevation, $z_\mathrm{H} = 1$ km, and the mean lowland elevation, $z_\mathrm{L} = -4$ km (Figure 2a). At the south pole the groundwater table is horizontal by symmetry and along the shoreline the head is prescribed, $h(\theta_\mathrm{o}) = h_o$. Integrating Equation (2) twice with these constraints, we obtain the following analytic solution for the head of the aquifer

$$h(\theta) = \sqrt{h_o^2 + 2\frac{rR^2}{K}\underbrace{\left[\ln\left|\frac{\sin\theta}{\sin\theta_\mathrm{o}}\right| - \cos\theta_r\ln\left|\frac{(\cos\theta+1)\sin\theta_\mathrm{o}}{(\cos\theta_\mathrm{o}+1)\sin\theta}\right|\right]}_{\Delta(\theta,\theta_r,\theta_\mathrm{o})}}. \tag{3}$$

This solution is valid for $\theta_r \leq \theta \leq \theta_\mathrm{o}$ and the solution for $\theta < \theta_r$ is constant at $h(\theta_r)$ as shown in Figures 2a-2c. Note that this solution assumes that recharge extends all the way to the shoreline, $\theta_\mathrm{o} \leq 180° - \theta_r$, a more general solution is given in the Section S3 of the supplementary information (SI). The expressions for specific and total discharge are given in the SI (Figure S2).

2.3 Numerical Model for southern highlands aquifer

To investigate the effects of complex shorelines and impact basins on plausible recharge rates, we have developed a numerical model for the southern highlands' aquifer. We nondimensionalize Equation (1) and discretize it in spherical shell geometry. The model uses conservative finite differences on a tensor product grid with an operator-based implementation (LeVeque, 1992). The resulting non-linear system of algebraic equations is solved with the Newton-Raphson method. The numerical implementation and benchmarking against the analytic solution are provided in SI Section S4.

To obtain the locations of the shorelines in the northern lowlands and basins, MOLA topography is down-sampled to our grid pixel resolution of 1.2°. By assuming an equipotential surface across a standing body of water, the shorelines are used to divide the computational domain into the southern highlands aquifer and three open water basins. The cells within these basins are excluded from the computations and the head in these basins is set to the chosen shoreline elevation. We also examine an aquifer domain that does not consider Hellas and Argyre basins.

All numerical solutions presented below assume a hydraulic conductivity of $K = 10^{-7}$ m/s and assume that all standing water bodies have elevations equal to the Arabia shoreline at -2090 m. Results for other shorelines are provided in the SI Section S5.3 and S5.4.

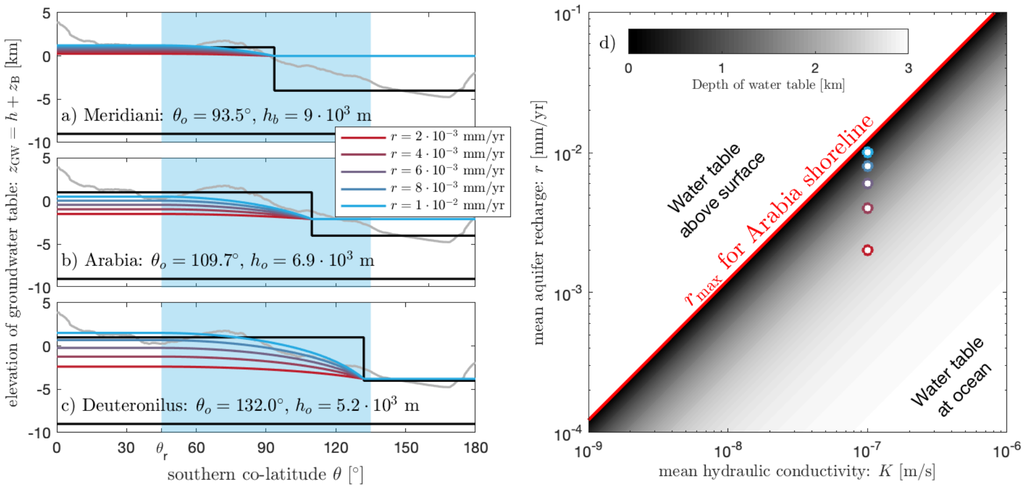

Figure 2. *a-c*) Analytic solution for steady unconfined aquifer on a spherical shell. Elevation of the groundwater table for the mean Meridiani, Arabia, and Deuteronilus shoreline elevations of Carr and Head, 2003. In each case, the groundwater table is shown for multiple values of recharge and the region receiving recharge is shaded blue. *d*) Depth of groundwater beneath mean highland elevation, $z_{\mathrm{H}} = 1$ km for the Arabia shoreline. The parameters corresponding to solutions from panel 2*b* are shown by correspondingly colored circles. The maximum plausible recharge from Equation (4) is shown in red.

3 Results

The analytical and numerical aquifer models introduced above provide complementary information about the plausible steady-state recharge values for Mars' southern highlands aquifer. The analytic solution gives insight into the relationship between recharge and hydraulic conductivity whereas the numerical results allow us to investigate the effects of complex shoreline geometry on recharge.

Neither the mean hydraulic conductivity nor the mean recharge of the southern highlands aquifer on Mars are known. Our analysis shows that the solution for the head, given by Equation (3), is primarily a function of the dimensionless ratio between recharge and hydraulic conductivity, r/K. This ratio then allows us to estimate which values of recharge are plausible given any proposed value of the mean hydraulic conductivity. For example, Figures 2*a*-2*c* show the elevation of the groundwater table in the spherical cap aquifer for different shorelines and increasing values of recharge. For the hydraulic conductivity of 10^{-7} m/s chosen here, the analytic model predicts values of recharge on the order of 10^{-3} mm/yr can raise the groundwater table to the surface using any chosen shoreline.

The absence of widespread groundwater upwelling outside Arabia Terra provides an upper bound on plausible r/K ratios. In our simplified analytic model widespread upwelling would occur if the elevation of the groundwater table exceeds the mean elevation of the highlands, assumed to be 1 km. From the analytic solution, this maximum ratio is given by

$$\left.\frac{r}{K}\right|_{\max} = \frac{d^2 - h_o^2}{2R^2 \Delta'(\theta_r, \theta_{\mathrm{o}})}, \tag{4}$$

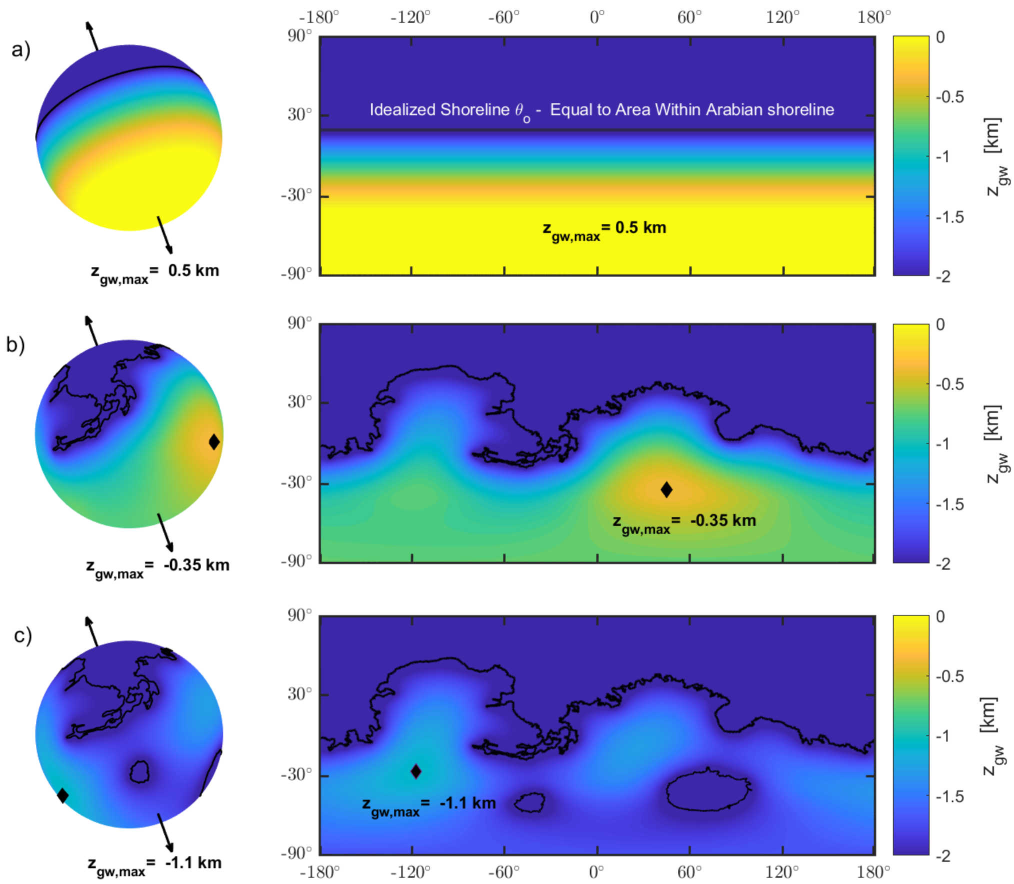

Figure 3. Effect of complex geometry for an aquifer with a recharge rate of 10^{-2} mm/yr evenly distributed between -45° and 45°: *a*) Analytic solution from Equation (3) with mean Arabia shoreline. *b*) Numerical solution with Arabia shoreline. *c*) Numerical solution with Arabia shoreline and standing water in Hellas and Argyre basins. Water elevation in the basins is assumed equal to the Arabia shoreline elevation.

where $\Delta'(\theta_r, \theta_o) = \Delta(\theta_r, \theta_r, \theta_o)$ is a scalar defined in Equation (3). Figure 2*d* shows the plausible combinations of hydraulic conductivity and recharge for the Arabia shoreline. This illustrates that dropping the mean K by an order of magnitude requires a similar drop in mean r to prevent widespread upwelling. The effects of varying other parameters, such as the chosen shoreline and the recharge distribution are minor and therefore presented in the SI (Section S3.3). For example, if the width of the recharge band, $\Delta\theta_r$, is varied by $\pm 20°$ around the preferred value of 90° for an aquifer with $K = 10^{-7}$ m/s the maximum plausible values of mean recharge for all three shorelines vary only between 6×10^{-3} and 1.6×10^{-2} mm/yr (Figure S3).

Analysis of the simplified spherical cap aquifer model demonstrates that the elevation of the groundwater table is primarily a function of the r/K ratio. Although the mean K of the southern highlands is not known, reasonable values in the range of 10^{-6} to 10^{-8} m/s (Hanna & Phillips, 2005) require very low rates of groundwater recharge to avoid widespread groundwater upwelling (Figure 2*d*). This conclusion is relatively insensitive to the particular shoreline chosen, the latitudinal width of the precipitation band, or the depth of the aquifer base. The particular value of the ratio r/K is primarily set by the large surface area of the highlands relative to the cross-sectional area of the aquifer, as discussed in Section 4.

To explore the effect of complex aquifer boundaries we present numerical solutions with the Arabia shoreline for $K = 10^{-7}$ m/s and $r = 10^{-2}$ mm/yr (Figure 3). First we explore the effect of the shoreline of the northern ocean alone and then consider the influence of adding Hellas and Argyre basins. Comparing the analytic solution for the spherical cap aquifer (Figure 3a) with the numerical solution for the Arabia shoreline (Figure 3b) we observe an overall drop in the elevation of the groundwater table. The complex shoreline generates a local maximum in the groundwater elevation at the furthest location from a shoreline within the precipitation band. The complex shoreline has an increased shoreline length and reduces the distance to drain into a basin which results in more effective drainage compared to the equivalent mean shoreline. The presence of large impact basins further lowers the head in the aquifer (Figure 3c). These basins provide additional shorelines within the highlands that help to drain the aquifer.

Overall, our numerical model demonstrates that complex shorelines lower the head in the aquifer and therefore increase the plausible value of mean recharge. However, these geometric effects do not change the order-of-magnitude of the plausible range of r/K. As such, the unknown mean hydraulic conductivity of the highlands remains the dominant control on the mean recharge. In Figure 4, we explore the location and extent of groundwater upwelling in the southern highlands as function of mean recharge in an aquifer bounded by the Arabia shoreline at the dichotomy and shorelines of equivalent elevation in Hellas and Argyre. Figure 4a-4c shows the depth, compared to topography, of the groundwater table for a succession of simulations with increasing amounts of recharge. Areas with blue colors are submerged while areas of incipient groundwater upwelling are shown in white. For $r = 10^{-2}$ mm/yr the highlands do not experience significant groundwater upwelling outside of some deep craters (Figure 4a), suggesting r is too low. Increasing recharge to 3×10^{-2} mm/yr a region of groundwater upwelling forms in Arabia Terra (Figure 4b), where geomorphic and geochemical observations suggest upwelling has occurred (e.g., McLennan et al., 2005; Grotzinger et al., 2005). A further increase in recharge to only 10^{-1} mm/yr results in large areas of the highlands becoming flooded, a scenario not supported by existing observations (Figure 4c), indicating that r is too high.

The area of the highlands that experiences groundwater upwelling grows rapidly with increasing recharge (Figure 4d). The geologic observation that groundwater upwelling has been restricted to primarily Arabia Terra therefore places a constraint on the plausible r/K ratio on Mars. For the mean hydraulic conductivity $K = 10^{-7}$ m/s, the best match with the inferred area of groundwater upwelling in Arabia Terra is a recharge of approximately 3×10^{-2} mm/yr, which leads to 6.3% of the highlands experiencing upwelling (Figure 4b). This corresponds to $r/K \sim 10^{-5}$ that can be used to estimate plausible values of r for any preferred value of K.

4 Discussion

Our results show that a groundwater aquifer beneath the highlands requires very low values of recharge to avoid groundwater upwelling occurring outside areas suggested by observational evidence. We show that the plausible steady-state recharge increases linearly with the assumed mean hydraulic conductivity of the aquifer. As such, plausible recharge values for any preferred hydraulic conductivity can be estimated as $r \sim 10^{-5}K$. This relationship is evident from the analytic solution (Equation 4) and confirmed by numerical models of varying complexity. Whereas the geometry of the shorelines has a small effect on the overall magnitude of recharge, Mars' topography requires upwelling to occur first in Arabia Terra as recharge rates increase, as indicated in previous work (Andrews-Hanna et al., 2007). If upwelling is constrained to Arabia Terra and the cho-

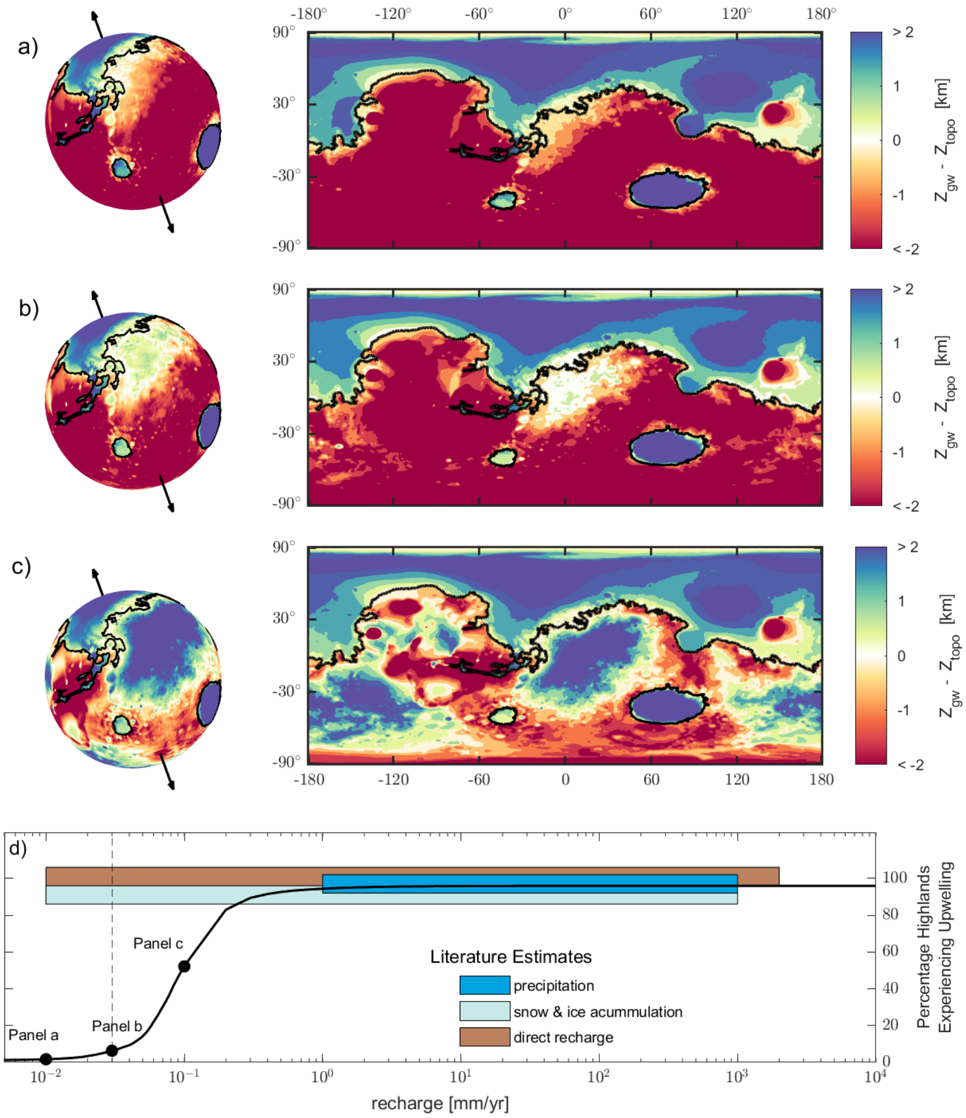

Figure 4. Groundwater upwelling as function of recharge for an aquifer bounded by the Arabia shoreline and equal elevation shorelines in Hellas and Argyre. Recharge, r, is evenly distributed between -45° and 45° and $K = 10^{-7}$ m/s. *a*) $r = 1 \times 10^{-2}$ mm/yr. *b*) $r = 3 \times 10^{-2}$ mm/yr. *c*) $r = 1 \times 10^{-1}$ mm/yr. *d*) Percentage of the southern highlands area experiencing groundwater upwelling as function of recharge with estimates of water availability (Stucky de Quay et al., 2021).

sen K value is held constant, the range of plausible recharge rates varies by less than one order of magnitude (Figure 4d)

Previous studies of global-scale groundwater flow estimate recharge rates from $\sim 10^{-2}$ mm/yr (Andrews-Hanna et al., 2007) to $\sim 10^{-1}$ mm/year (Andrews-Hanna & Lewis, 2011) for comparable mean hydraulic conductivities, see SI Section S5.1. These estimates are consistent with our results and suggest that they are not strongly dependent on model assumptions. For example, previous models do not allow for ponded surface water and the resulting shorelines. In our model recharge is prescribed as an input where in previous work it is calculated as a dynamic output. Finally, we assume a constant hydraulic conductivity, while previous models apply a decay of permeability with depth. Despite these differences, our recharge estimates are comparable.

We suggest that these low values of mean recharge are simply due to the large surface area, A_s, of the aquifer relative to its small cross-sectional area, A_x. This geometric control can be understood by a volume balance over a spherical cap aquifer at steady state. The total rate of recharge is $Q_r = A_s r$ and the total discharge out of the aquifer is $Q_d = A_\mathrm{x} q_\theta$, where q_θ is volumetric flux from Darcy's law. Total volume balance requires that $Q_d = Q_r$, so that

$$\frac{r}{K} = \frac{A_\mathrm{x}}{A_s}\mathrm{q}_\theta \sim \frac{d\Delta h}{R^2} \sim 10^{-5}, \tag{5}$$

where $R \sim 10^6$ m is the radius of Mars, $d \sim 10^4$ m is the thickness of the aquifer and $\Delta h \sim 10^3$ m is the elevation change of the groundwater table across the aquifer. Here we have approximated $A_s \sim R^2$ and $A_\mathrm{x} \sim R$ and Darcy's law as $q_\theta \sim K\Delta h/R$. This simple estimate is identical to the r/K ratio obtained from the analytic solution and computed from the numerical models. For a detailed discussion of the total volume balance see SI Section S1.

While previous work has computed specific values of recharge for specific model parameters, our contribution demonstrates the linear relation between r and K that allows estimates of plausible steady recharge for any presumed value of K. This is valuable precisely because K is highly uncertain and the linear relationship allows investigation of different scenarios. For example, consider a steady hydrologic cycle where a significant fraction of the precipitation infiltrates and recharges the aquifer, but groundwater upwelling is limited to Arabia Terra. To align with published precipitation estimates, this scenario would require an increase in recharge by almost two orders of magnitude (Figure 4d). The linear relation between r and K would thus require a two order of magnitude increase in the mean conductivity of the aquifer to keep upwelling restricted to Arabia Terra.

While local variations in K by several orders of magnitude are not unusual, the K in our equations is the average over the entire aquifer. This average includes rapid decay of the conductivity with depth. As such, it is much less likely that the mean K of the aquifer would increase to the value of 10^{-5} m/s, required to make recharge comparable to precipitation estimates of more than 1 mm/yr. If conductivity is lower, than assumed here and in previous work (Clifford, 1993b; Clifford & Parker, 2001; Hanna & Phillips, 2005), the r/K-relation requires that groundwater recharge in a steady hydrologic cycle is orders of magnitude less than published precipitation estimates (Kamada et al., 2020; Wordsworth et al., 2015). The difference between estimates of precipitation and groundwater recharge requires that most precipitation becomes overland flow and run off. This implies that surface and subsurface hydrology are only weakly coupled in this particular scenario.

All of the above considerations assume a steady hydrological system, because the the model presented here is at steady state. However, Mars hydrological activity is generally thought to occur during short climatic excursions that produce conditions favorable for precipitation (Grotzinger et al., 2014; Wordsworth et al., 2015). In this context, our recharge estimates should be interpreted as average over hydrologically active and inactive periods. As such, the recharge during the active periods may exceed the steady-state values.

The transient response of the groundwater table to individual ephemeral precipitation events is another possible explanation for the low calculated mean recharge values when compared to previous estimates (Figure 4d). If the transient response time of the aquifer is longer than the timescale of climate excursions producing larger values of recharge, the groundwater table may not breach the surface before the excursion ends and recharge declines. The transient aquifer response will be examined in future work, but this response is likely dependent on initial water table elevations at the beginning of a given climate excursion.

One other consideration is Mars' total water budget, and how that compares to water volumes in our model simulations. With the Arabia Terra shoreline, and our preferred recharge value of $3{\times}10^{-}2$ mm/yr, the total volume of water contained in the Mars southern highlands aquifer is ~ 670 m GEL (global equivalent layer) see SI Section S5.2 for calculation. This is a median value when compared to literature values ranging from 100 to 1500 m (e.g., Scheller et al., 2021). If the overall water volumes of Mars are sufficient to form standing bodies of surface water, as reflected by the proposed shorelines, then our results show that even very low rates of background groundwater recharge would be sufficient to elevate the water table. This would result in high groundwater tables at the beginning of a climate excursion and may limit the amount of transient recharge possible to avoid a wide-spread upwelling scenario.

5 Conclusions

Our analytical and numerical solutions for the Martian highlands aquifer show that the elevation of the groundwater table is controlled by the ratio of the mean recharge to the mean hydraulic conductivity of the aquifer. This allows estimates of plausible recharge rates given any preferred aquifer conductivity. For commonly assumed conductivities of $\sim 10^{-7}$ m/s (permeability $\sim 10^{-14}$ m^2) the mean groundwater recharge on the highlands is $\sim 10^{-2}$ mm/yr. This value is at the low end of previously proposed estimates of aquifer recharge and two orders-of-magnitude below estimates of precipitation. If the hydrologic cycle is at steady-state and published precipitation estimates are correct, then our groundwater models imply that most precipitation must form runoff.

6 Open Research

The code is currently available on Github (`https://github.com/ehiatt/Limited-Recharge-of-a-Deep-Groundwater-Aquifer-In1-the-Southern-Highlands-of-Early-Mars`). The final version of the code will be uploaded to Zenodo after the review process has completed.

Acknowledgments

M.A.H. acknowledges support from NASA Emerging World Grant number 18−EW18_2−0027. E.H acknowledges support from the Gale White Fellowship from the University of Texas Institute for Geophysics (UTIG), #XXXX, and the Fellowship in Planetary Habitability from the Center for Planetary Systems Habitability (CPSH), #XXXX.

References

Andrews-Hanna, & Lewis. (2011). Early Mars hydrology: 2. Hydrological evolution in the Noachian and Hesperian epochs. *Journal of Geophysical Research E: Planets*, *116*(2), 1–20. doi: 10.1029/2010JE003709

Andrews-Hanna, Phillips, R. J., & Zuber, M. T. (2007). Meridiani Planum and the global hydrology of Mars. *Nature*, *446*(7132), 163–166. doi: 10.1038/nature05594

Andrews-Hanna, Zuber, M. T., Arvidson, R. E., & Wiseman, S. M. (2010). Early Mars hydrology: Meridiani playa deposits and the sedimentary record of Arabia Terra. *Journal of Geophysical Research E: Planets*, *115*(6), 1–22. doi: 10.1029/2009JE003485

Batchelor, G. (2000). *An Introduction to Fluid Dynamics.* Cambridge University Press.

Bibring, J.-P., Arvidson, R., Gendrin, A., Gondet, B., Langevin, Y., Le Mouelic, S., ... others (2007). Coupled ferric oxides and sulfates on the martian surface. *science*, *317*(5842), 1206–1210.

Boussinesq, J. (1903). *Théorie Analytique de la Chaleur.* Paris: Gauthier-Villars.

Cabrol, N. A., & Grin, E. A. (1999). Distribution, classification, and ages of martian impact crater lakes. *Icarus*, *142*(1), 160–172.

Carr, M. H. (1986). Mars: A water-rich planet? *Icarus*, *68*(2), 187–216.

Carr, M. H. (1996). Water on mars. *New York: Oxford University Press*.

Carr, M. H., & Head, J. W. (2003). Oceans on Mars: An assessment of the observational evidence and possible fate. *Journal of Geophysical Research E: Planets*, *108*(5), 1–28. doi: 10.1029/2002je001963

Carter, J., Poulet, F., Bibring, J.-P., Mangold, N., & Murchie, S. (2013). Hydrous minerals on mars as seen by the crism and omega imaging spectrometers: Updated global view. *Journal of Geophysical Research: Planets*, *118*(4), 831–858.

Chan, N.-H., Perron, J. T., Mitrovica, J. X., & Gomez, N. A. (2018). New evidence of an ancient martian ocean from the global distribution of valley networks. *Journal of Geophysical Research: Planets*, *123*(8), 2138–2150.

Christensen, P. R., Bandfield, J., Clark, R., Edgett, K., Hamilton, V., Hoefen, T., ... others (2000). Detection of crystalline hematite mineralization on mars by the thermal emission spectrometer: Evidence for near-surface water. *Journal of Geophysical Research: Planets*, *105*(E4), 9623–9642.

Citron, R. I., Manga, M., & Hemingway, D. J. (2018). Timing of oceans on mars from shoreline deformation. *Nature*, *555*(7698), 643–646.

Clifford, S. (1993a). A model for the hydrologic and climatic behavior of water on mars. *Journal of Geophysical Research: Planets*, *98*(E6), 10973–11016.

Clifford, S. (1993b). A model for the hydrologic and climatic behavior of water on Mars. *Journal of Geophysical Research*, *98*(E6), 10973–11016. doi: 10.1029/93je00225

Clifford, S., & Parker, T. (2001). The evolution of the martian hydrosphere: Implications for the fate of a primordial ocean and the current state of the northern plains. *Icarus*, *154*(1), 40–79.

Davis, J., Balme, M., Grindrod, P., Williams, R., & Gupta, S. (2016). Extensive noachian fluvial systems in arabia terra: Implications for early martian climate. *Geology*, *44*(10), 847–850.

Di Achille, G., & Hynek, B. M. (2010). Ancient ocean on mars supported by global distribution of deltas and valleys. *Nature Geoscience*, *3*(7), 459–463.

Dohm, J., Hare, T., Robbins, S., Williams, J.-P., Soare, R., El-Maarry, M. R., ... others (2015). Geological and hydrological histories of the argyre province, mars. *Icarus*, *253*, 66–98.

Dupuit, J. (1863). *Etudes théoriques et pratiques sur le mouvement des eaux dans les canaux découverts et àtravers les terrains perméable* (2nd ed.). Paris: Dunod.

Ehlmann, B. L., Mustard, J. F., Swayze, G. A., Clark, R. N., Bishop, J. L., Poulet, F., ... others (2009). Identification of hydrated silicate minerals on mars using mro-crism: Geologic context near nili fossae and implications for aqueous alteration. *Journal of Geophysical Research: Planets*, *114*(E2).

Fassett, C., & Head, J. W. (2008a). The timing of martian valley network activity:

Constraints from buffered crater counting. *Icarus*, *195*(1), 61–89.
Fassett, C., & Head, J. W. (2008b). Valley network-fed, open-basin lakes on mars: Distribution and implications for noachian surface and subsurface hydrology. *Icarus*, *198*(1), 37–56.
Fastook, J. L., & Head, J. W. (2015). Glaciation in the late noachian icy highlands: Ice accumulation, distribution, flow rates, basal melting, and top-down melting rates and patterns. *Planetary and Space Science*, *106*, 82-98. Retrieved from `https://www.sciencedirect.com/science/article/pii/S0032063314003924` doi: https://doi.org/10.1016/j.pss.2014.11.028
Forchheimer, P. (1901). Wasserbewegung durch Boden. *Zeitschrift des Vereins Deutscher Ingenieure*, *45*, 1782–1788.
Frey, H. (2008). Ages of very large impact basins on Mars: Implications for the late heavy bombardment in the inner solar system. *Geophysical Research Letters*, *35*(13), 1–4. doi: 10.1029/2008GL033515
Goldspiel, J. M., & Squyres, S. W. (1991). Ancient aqueous sedimentation on mars. *Icarus*, *89*(2), 392–410.
Golombek, M., Grant, J. A., Parker, T., Kass, D., Crisp, J., Squyres, S. W., . . . others (2003). Selection of the mars exploration rover landing sites. *Journal of Geophysical Research: Planets*, *108*(E12).
Grotzinger, J. P., Arvidson, R., Bell Iii, J., Calvin, W., Clark, B., Fike, D., . . . others (2005). Stratigraphy and sedimentology of a dry to wet eolian depositional system, burns formation, meridiani planum, mars. *Earth and Planetary Science Letters*, *240*(1), 11–72.
Grotzinger, J. P., Sumner, D. Y., Kah, L., Stack, K., Gupta, S., Edgar, L., . . . others (2014). A habitable fluvio-lacustrine environment at yellowknife bay, gale crater, mars. *Science*, *343*(6169), 1242777.
Hanna, & Phillips, R. J. (2005). Hydrological modeling of the Martian crust with application to the pressurization of aquifers. *Journal of Geophysical Research E: Planets*, *110*(1), 1–19. doi: 10.1029/2004JE002330
Hargitai, H. I., Gulick, V. C., & Glines, N. H. (2018). Paleolakes of northeast hellas: Precipitation, groundwater-fed, and fluvial lakes in the navua–hadriacus–ausonia region, mars. *Astrobiology*, *18*(11), 1435–1459.
Harrison, K. P., & Grimm, R. E. (2009, 4). Regionally compartmented groundwater flow on Mars. *Journal of Geophysical Research E: Planets*, *114*(4). doi: 10.1029/2008JE003300
Hiesinger, H., & Head, J. W. (2002). Topography and morphology of the argyre basin, mars: implications for its geologic and hydrologic history. *Planetary and Space Science*, *50*(10-11), 939–981.
Hoke, M. R., Hynek, B. M., & Tucker, G. E. (2011). Formation timescales of large martian valley networks. *Earth and Planetary Science Letters*, *312*(1-2), 1–12.
Horvath, D. G., & Andrews-Hanna, J. C. (2017). Reconstructing the past climate at gale crater, mars, from hydrological modeling of late-stage lakes. *Geophysical Research Letters*, *44*(16), 8196–8204.
Hynek, B. M., & Phillips, R. J. (2001). Evidence for extensive denudation of the martian highlands. *Geology*, *29*(5), 407–410.
Kamada, A., Kuroda, T., Kasaba, Y., Terada, N., Nakagawa, H., & Toriumi, K. (2020). A coupled atmosphere–hydrosphere global climate model of early mars: A 'cool and wet' scenario for the formation of water channels. *Icarus*, *338*, 113567. Retrieved from `https://www.sciencedirect.com/science/article/pii/S0019103518300927` doi: https://doi.org/10.1016/j.icarus.2019.113567
LeVeque, R. (1992). *Numerical Methods for Conservation Laws.* Birkhaeuser Verlag.
Luo, W., Grudzinski, B., & Pederson, D. (2011). Estimating hydraulic conductivity for the martian subsurface based on drainage patterns—a case study in the mare tyrrhenum quadrangle. *Geomorphology*, *125*(3), 414–420.

Luo, W., & Howard, A. (2008, 5). Computer simulation of the role of groundwater seepage in forming Martian valley networks. *Journal of Geophysical Research*, *113*(E5), E05002. Retrieved from `http://doi.wiley.com/10.1029/2007JE002981` doi: 10.1029/2007JE002981

Malin, M. C., & Edgett, K. S. (1999). Oceans or seas in the martian northern lowlands: High resolution imaging tests of proposed coastlines. *Geophysical Research Letters*, *26*(19), 3049–3052.

McLennan, S. M., Bell Iii, J., Calvin, W., Christensen, P., Clark, B. d., De Souza, P., ... others (2005). Provenance and diagenesis of the evaporite-bearing burns formation, meridiani planum, mars. *Earth and Planetary Science Letters*, *240*(1), 95–121.

Milton, D. J. (1973). Water and processes of degradation in the martian landscape. *Journal of Geophysical Research*, *78*(20), 4037–4047.

Mustard, J. F., Murchie, S. L., Pelkey, S., Ehlmann, B., Milliken, R., Grant, J. A., ... others (2008). Hydrated silicate minerals on mars observed by the mars reconnaissance orbiter crism instrument. *Nature*, *454*(7202), 305–309.

Parker, T., Clifford, S., & Banerdt, W. (2000). Argyre planitia and the mars global hydrologic cycle. In *Lunar and planetary science conference* (p. 2033).

Parker, T., Gorsline, D., Saunders, R., Pieri, D. C., & Schneeberger, D. M. (1993). Coastal geomorphology of the Martian northern plains. *Journal of Geophysical Research*, *98*(E6), 11061–11078. Retrieved from `http://doi.wiley.com/10.1029/93JE00618` doi: 10.1029/93JE00618

Parker, T., Saunders, S., & Schneeberger, D. (1989). Transitional morphology in west deuteronilus mensae, mars: Implications for modification of the lowland/upland boundary. *Icarus*, *82*(1), 111–145.

Perron, J., Mitrovica, J., Manga, M., Matsuyama, I., & Richards, M. (2007). Evidence for an ancient martian ocean in the topography of deformed shorelines. *Nature*, *447*(7146), 840–843. doi: 10.1038/nature05873

Ramirez, R. M., Craddock, R. A., & Usui, T. (2020). Climate simulations of early mars with estimated precipitation, runoff, and erosion rates. *Journal of Geophysical Research: Planets*, *125*(3), e2019JE006160.

Salese, F., Pondrelli, M., Neeseman, A., Schmidt, G., & Ori, G. G. (2019). Geological evidence of planet-wide groundwater system on mars. *Journal of Geophysical Research: Planets*, *124*(2), 374–395.

Scheller, E., Ehlmann, B., Hu, R., Adams, D., & Yung, Y. (2021). Long-term drying of mars by sequestration of ocean-scale volumes of water in the crust. *Science*, *372*(6537), 56–62.

Shadab, M., Hiatt, E., & Hesse, M. (2022). Estimates of martian mean recharge rates from analytic groundwater models. *LPI Contributions*, *2678*, 1775.

Sholes, S. F., Dickeson, Z. I., Montgomery, D. R., & Catling, D. C. (2021). Where are mars' hypothesized ocean shorelines? large lateral and topographic offsets between different versions of paleoshoreline maps. *Journal of Geophysical Research: Planets*, *126*(5), e2020JE006486.

Sholes, S. F., Montgomery, D. R., & Catling, D. C. (2019). Quantitative high-resolution reexamination of a hypothesized ocean shoreline in cydonia mensae on mars. *Journal of Geophysical Research: Planets*, *124*(2), 316–336.

Sholes, S. F., & Rivera-Hernández, F. (2022). Constraints on the uncertainty, timing, and magnitude of potential mars oceans from topographic deformation models. *Icarus*, *378*, 114934. Retrieved from `https://www.sciencedirect.com/science/article/pii/S0019103522000550` doi: https://doi.org/10.1016/j.icarus.2022.114934

Smith, D. E., Zuber, M. T., Solomon, S. C., Phillips, R. J., Head, J. W., Garvin, J. B., ... others (1999). The global topography of mars and implications for surface evolution. *science*, *284*(5419), 1495–1503.

Squyres, S. W., Grotzinger, J. P., Arvidson, R. E., Bell III, J. F., Calvin, W., Christensen, P. R., ... others (2004). In situ evidence for an ancient aqueous environment at meridiani planum, mars. *science*, *306*(5702), 1709–1714.

Stucky de Quay, G., Goudge, T. A., Kite, E. S., Fassett, C. I., & Guzewich, S. D. (2021). Limits on runoff episode duration for early mars: Integrating lake hydrology and climate models. *Geophysical Research Letters*, *48*(15), e2021GL093523.

von Paris, P., Petau, A., Grenfell, J., Hauber, E., Breuer, D., Jaumann, R., ... Tirsch, D. (2015). Estimating precipitation on early mars using a radiative-convective model of the atmosphere and comparison with inferred runoff from geomorphology. *Planetary and Space Science*, *105*, 133-147. Retrieved from `https://www.sciencedirect.com/science/article/pii/S0032063314003778` doi: https://doi.org/10.1016/j.pss.2014.11.018

Werner, S. (2008). The early martian evolution—constraints from basin formation ages. *Icarus*, *195*(1), 45–60.

Wilson, S. A., Moore, J. M., Howard, A. D., & Wilhelms, D. E. (2010). Evidence for ancient lakes in the hellas region. *Lakes on Mars*, 195–222.

Wordsworth, R. D., Kerber, L., Pierrehumbert, R. T., Forget, F., & Head, J. W. (2015, 6). Comparison of "warm and wet" and "cold and icy" scenarios for early Mars in a 3-D climate model. *Journal of Geophysical Research: Planets*, *120*(6), 1201–1219. Retrieved from `http://doi.wiley.com/10.1002/2015JE004787` doi: 10.1002/2015JE004787

Zhao, J., Xiao, L., & Glotch, T. D. (2020). Paleolakes in the northwest hellas region, mars: Implications for the regional geologic history and paleoclimate. *Journal of Geophysical Research: Planets*, *125*(3), e2019JE006196.